A Novel Dual-Stator Hybrid Excited Synchronous Wind Generator

Xiping Liu, Heyun Lin, Z. Q. Zhu, *Fellow, IEEE*, Chengfeng Yang, Shuhua Fang, and Jian Guo

***Abstract*—This paper presents a novel dual-stator hybrid excited synchronous wind generator and describes its structural features and operation principle. The no-load magnetic fields with different field currents are computed by 3-D finite-element method. Static characteristics, including the flux-linkage and EMF waveforms of stator windings, and inductance waveforms of armature windings and field winding, are analyzed. The simulation results show that due to the dual-stator structure, the air-gap magnetic flux can be easily controlled, while the output voltage can be increased effectively. Tests are performed on the prototype machine to validate the predicted results, and an excellent agreement is obtained.**

***Index Terms*—Air-gap flux, dual stator, finite-element method (FEM), hybrid excited.**

I. Introduction

HYBRID excitation synchronous machines (HESMs) have recently been the subject of extensive research since they combine the advantages of permanent-magnet (PM) machines with the possibility of controlling air-gap magnetic flux easily by auxiliary windings. They are eminently suitable for applications which require constant voltage power generation and wide-speed constant power operation.

Many topologies of HESMs have been proposed for wide-speed constant power operation. They may be grouped into four types: hybrid excitation doubly salient machine [1], [2], consequent pole PM machine (CPPM) [3], brushless PM hybrid machine with a claw-pole-type rotor [4], and homopolar and bipolar HESMs [5].

CPPM can also be used for constant voltage power generation [6], in which an excitation coil is placed on the outer stator. However, its relatively long excitation coil per turn may lead to high excitation loss. Compared with CPPM, hybrid excitation claw-pole rotor generator can maintain its output voltage constant by employing relatively low excitation current, but the leakage flux is much more significant [7]. In order to reduce the leakage flux, the hybrid excitation synchronous generator installs the PMs and excitation coils on the shaft independently [8]. The leakage flux can also be reduced in a double-disc generator [9]. In addition, a hybrid excitation synchronous generator is developed for automotive applications [10], but it has brushes and slip rings. However, up to date, there is no report that HESM is applied to the wind power generation system.

The concept of double-stator cup-rotor PM machine has been introduced to perform the flux control [11], while other types of double-stator machines have been applied to maintain the output voltage in the wind power generation [12], to increase the starting torque [13], [14], and to compensate energy [15] of electric vehicles. The double-stator structure should be able to improve power density when it is used in the wind power generation.

As it is well known, in general, the diameter of wind power generator is large and the power density is low due to low wind speed. Moreover, the output voltage of wind generator often varies with the wind speed or load. The purpose of this paper is to present a novel dual-stator hybrid excited synchronous wind generator (DSHESG) to overcome these shortcomings. The structural features and operation principle of DSHESG will be described, and some static characteristics will be obtained by the finite-element analysis (FEA). A prototype of DSHESG is manufactured, and its no-load performance and phase EMF are measured. The FEA result of the prototype is in excellent agreement with the experimental measurement. It is also shown that the power density and the output voltage of DSHESG can be effectively increased by using an inner stator.

II. Structure and Operation Principle of DSHESG

A. Structure of DSHESG

Fig. 1, together with Figs. 2 and 5(a), as will be shown later, shows the structure of the proposed DSHESG, which mainly consists of PMs, claw poles, field winding, outer stator, inner stator, rotor yoke, cup rotor, brackets of inner stator and field winding, etc. The stator is composed of outer stator, inner stator, field winding, etc., and the rotor consists of the PMs, claw poles, rotor yoke, and cup rotor. The PMs and claw poles share with the outer stator, and the inner stator is fixed on the shell of

Paper 2008-EMC-089, presented at the 2007 International Conference on Power Electronics and Drives Systems, Bangkok, Thailand, November 27–30, and approved for publication in the IEEE Transactions on Industry Applications by the Electric Machines Committee of the IEEE Industry Applications Society. Manuscript submitted for review May 3, 2008 and released for publication November 25, 2008. Current version published May 20, 2009. This work was supported by the National Natural Science Foundation of China under Grant 50337030.

X. Liu, H. Lin, C. Yang, and S. Fang are with the School of Electrical Engineering, Southeast University, Nanjing 210096, China (e-mail: liuxp211@163.com; seueelab_lxp@163.com; hyling@seu.edu.cn; seueelab_ycf@163.com; sd_fsh@163.com; jn_fsh@sina.com).

Z. Q. Zhu is with the Department of Electronic and Electrical Engineering, University of Sheffield, Sheffield, S1 3JD, U.K. (e-mail: Z.Q.Zhu@sheffield.ac.uk).

J. Guo was with the School of Electrical Engineering, Southeast University, Nanjing 210096, China. He is now with the College of Automation Engineering, Nanjing University of Aeronautics and Astronautics, Nanjing 210016, China (e-mail: fossiler@163.com).

Color versions of one or more of the figures in this paper are available online at http://ieeexplore.ieee.org.

Digital Object Identifier 10.1109/TIA.2009.2018969

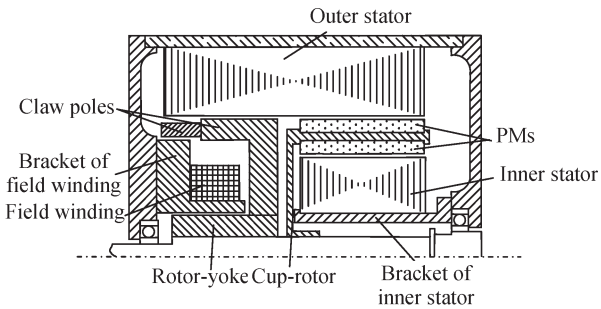

Fig. 1. Structure of DSHESG.

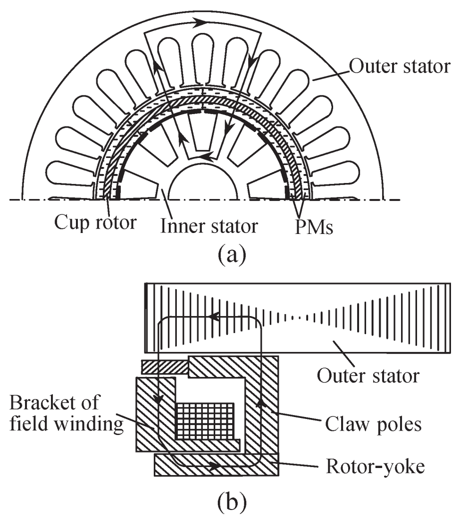

Fig. 2. Magnetic circuit of DSHESG. (a) PM. (b) DC field winding.

the machine. The field winding is also fixed on the shell of the machine by the bracket.

There are two magnetic circuits in the DSHESG, as shown in Fig. 2. One is PM magnetic circuit mainly consisting of PMs, air gap, cup rotor, and laminated stator core [see Fig. 2(a)], and the other is dc field magnetic circuit mainly including claw poles, air gap, laminated core of the outer stator, and bracket of field winding [see Fig. 2(b)]. Two magnetic circuits are in parallel independently. The PMs are fixed on the surface of the cup rotor, and the outer PMs are in series with the inner PMs in magnetic circuit.

Fig. 3(a) and (b) shows the corresponding equivalent magnetic circuits of PM and dc field winding, respectively, when the magnetic leakage flux is neglected.

The symbols in Fig. 3 are listed as follows.

F_{m1_out} and F_{m2_out}	MMFs of the outer PMs.
F_{m1_in} and F_{m2_in}	MMFs of the inner PMs.
R_{m1_out} and R_{m2_out}	Reluctances of two outer PMs.
R_{m1_in} and R_{m2_in}	Reluctances of two inner PMs.
R_{s_out} and R_{s_in}	Iron reluctances of the outer and inner stators.
$R_{\delta 1\_\mathrm{out}}$ and $R_{\delta 2\_\mathrm{out}}$	Air-gap reluctances between the outer stator and the outer PMs.
$R_{\delta 1\_\mathrm{in}}$ and $R_{\delta 2\_\mathrm{in}}$	Air-gap reluctances between the inner stator and the inner PMs.
ϕ_{o_pm} and ϕ_{i_pm}	Magnetic fluxes generated by the outer and the inner PMs.

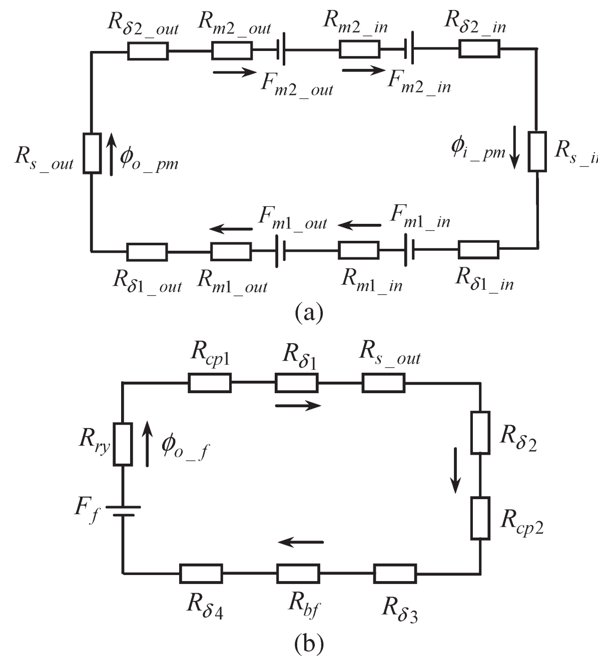

Fig. 3. Equivalent magnetic circuits of DSHESG. (a) PM. (b) DC field winding.

F_f	MMF of the field winding.
R_{cp1} and R_{cp2}	Reluctances of the two claw poles.
R_{ry}	Reluctance of the rotor yoke.
R_{bf}	Reluctance of bracket of the field winding.
$R_{\delta k}$	Air-gap reluctance.
ϕ_{o_f}	Magnetic flux generated by the field winding.

In the DSHESG, the MMF generated by PMs is constant, while that created by the field winding varies with the applied field current.

B. Operation Principle of DSHESG

The resultant phase EMF of DSHESG is the sum of three components

$$E_{\mathrm{sum}} = E_{i\_\mathrm{pm}} + E_{o\_\mathrm{pm}} + E_{o\_f} \tag{1}$$

where E_{i_pm} and E_{o_pm} are the induced EMFs in the inner and outer stator windings by PMs, respectively, while E_{o_f} is the induced EMF in the outer stator winding by the field winding.

Similarly, the total output power of the DSHESG can also be calculated by

$$P_{\mathrm{sum}} = P_{i\_\mathrm{pm}} + P_{o\_\mathrm{pm}} + P_{o\_f} \tag{2}$$

where P_{i_pm} and P_{o_pm} represent the powers which are produced in the inner and outer stators due to the PMs, respectively, while P_{o_f} is the power generated in the outer stator due to the field winding. They are related by the following ratio coefficients:

$$K_{p1} = \frac{P_{i\_\mathrm{pm}}}{P_{o\_\mathrm{pm}}} \quad K_{p2} = \frac{P_{o\_\mathrm{pm}}}{P_{o\_f}}. \tag{3}$$

In general, the phase EMF E and power P of an ac electrical machine are related by

$$E = 4K_B f K_w N\phi \tag{4}$$

$$P = mEI \tag{5}$$

where N is the number of series turns per phase, f denotes the frequency in hertz, K_w is the winding factor, K_B is the waveform factor of air-gap magnetic field, ϕ is the magnetic flux per pole, m represents the phase number, and I is the rms of phase current. Therefore, K_{p1} can be rewritten as

$$K_{p1} = \frac{P_{i\_\mathrm{pm}}}{P_{o\_\mathrm{pm}}} = \frac{mE_{i\_\mathrm{pm}} I_i}{mE_{o\_\mathrm{pm}} I_o} \tag{6}$$

where I_i and I_o are the phase currents of the inner and outer stators, respectively. Because the phase windings of the outer stator are in series with those of the inner stator, hence $I_i = I_o$. Therefore, by combining (4)–(6), the following expression can be obtained:

$$K_{p1} = \frac{4K_{B1} f K_{w1} N_i \phi_{i\_\mathrm{pm}}}{4K_{B2} f K_{w2} N_o \phi_{o\_\mathrm{pm}}} = \frac{K_{B1} K_{w1} N_i \phi_{i\_\mathrm{pm}}}{K_{B2} K_{w2} N_o \phi_{o\_\mathrm{pm}}} \tag{7}$$

where N_i and N_o, K_{w1} and K_{w2}, K_{B1} and K_{B2}, and ϕ_{i_pm} and ϕ_{o_pm} are the number of series turns per phase, the stator winding factors, the air-gap magnetic field waveform factors, and the magnetic fluxes per pole of the inner and outer stators due to PMs, respectively. Since the pole numbers of the outer and inner stators are the same and the magnetic circuits of PMs are in series, i.e., $\phi_{i\_\mathrm{pm}} = \phi_{o\_\mathrm{pm}}$, and N_i can be calculated by

$$N_i = \frac{K_{B2} K_{w2} N_o}{K_{B1} K_{w1}} K_{p1} \tag{8}$$

the power ratio coefficient K_{p2} can be rewritten as

$$\begin{aligned} K_{p2} &= \frac{E_{o\_\mathrm{pm}} I_o}{E_{o\_f} I_o} = \frac{E_{o\_\mathrm{pm}}}{E_{o\_f}} \\ &= \frac{4K_{B2} f K_{w2} N_o \phi_{o\_\mathrm{pm}}}{4K_{B2} f K_{w2} N_o \phi_{o\_f}} = \frac{\phi_{o\_\mathrm{pm}}}{\phi_{o\_f}} \end{aligned} \tag{9}$$

where ϕ_{o_f} is the magnetic flux per pole of the outer stator generated by the field winding. Once K_{p2} is known, ϕ_{o_f} can be determined by

$$\phi_{o\_f} = \frac{\phi_{o\_\mathrm{pm}}}{K_{p2}}. \tag{10}$$

In fact, ϕ_{o_f} can also be calculated by

$$\phi_{o\_f} = \frac{F_f}{R_f} = \frac{N_f i_f}{R_f} \tag{11}$$

where N_f is the number of turns of the field winding, i_f is the field current, and R_f is the reluctance of the dc field magnetic circuit. Combining (9)–(11), N_f can be calculated by

$$N_f = R_f \frac{\phi_{o\_\mathrm{pm}}}{K_{p2} i_f}. \tag{12}$$

TABLE I
SPECIFICATION AND DESIGN PARAMETERS OF A DSHESG

Item	Value	Item	Value
Rated speed (rpm)	400	Rated voltage (V)	120
Length of air gap(mm)	0.7	Pole number	8
PM remanence (T)	1.15	Core length of outer stator (mm)	164
PM coercivity(kA/m)	835	Core length of inner stator (mm)	70

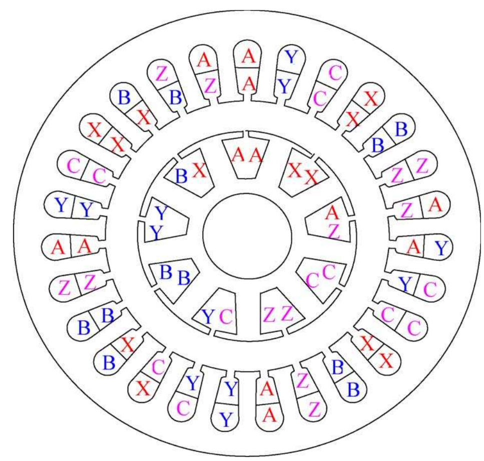

Fig. 4. Layout of armature windings.

C. Parameters of DSHESG

Table I shows the specification and design parameters of a prototype DSHESG. The slot numbers of outer stator and inner stators are 27 and 9, respectively.

Fig. 4 shows the layout of the armature windings. In order to reduce the cogging torque, the double-layer and short-pitch distributed windings are adopted for the outer stator, while the concentrated windings are adopted for the inner stator since the slot number of the inner stator is low. In the prototype DSHESG, K_{w1} of the inner stator is 0.975, and K_{w2} of the outer stator is 0.94. $N_o = 540$ and $N_i = 114$. Thus, K_{p1} can be calculated by (8), being 0.22.

III. MAGNETIC FIELD ANALYSIS AND STATIC CHARACTERISTICS

A. Magnetic Field Analysis

In the DSHESG, there are axial and radial magnetic circuits; 3-D finite-element method (FEM) is used to analyze its magnetic field distributions. Fig. 5 shows the corresponding 3-D FEA structural models and meshes.

The air-gap magnetic flux distributions obtained by the 3-D FEM analysis on the surface of claw poles and PMs over one pole region are shown in Fig. 6. Comparing Fig. 6(a) with Fig. 6(c), with negative field current excitations, the air-gap flux distributions on the surface of claw poles are obviously different, while those on the surface of PMs almost have no change. In addition, the flux density on the surface of claw poles is

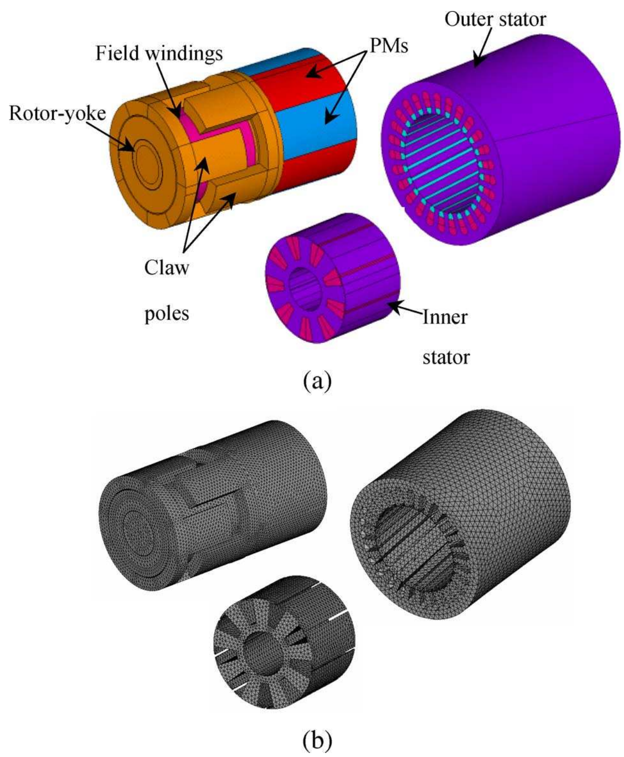

Fig. 5. Three-dimensional FEA. (a) Structural model. (b) Meshes.

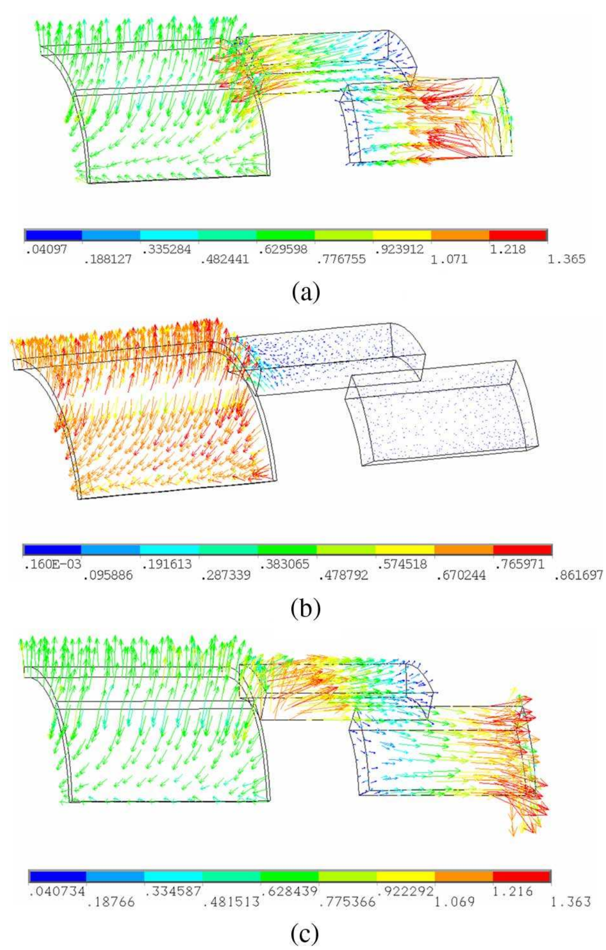

Fig. 6. Magnetic flux distribution in air gap. (a) $I = -0.5$ A. (b) $I = 0$. (c) $I = 0.5$ A.

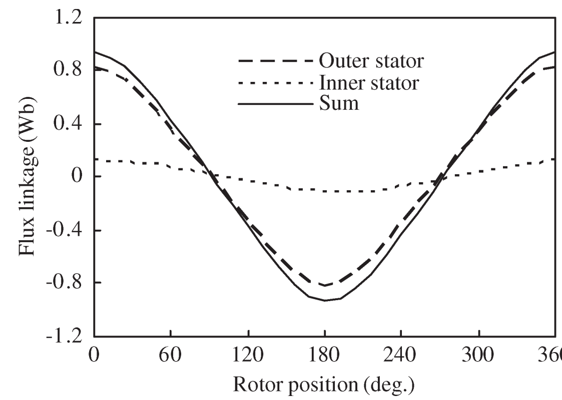

Fig. 7. Flux linkages.

nearly zero when no field current is applied, as shown in Fig. 6(b).

B. Static Characteristics

The flux linkages of two stator windings without field current excitation are calculated by 3-D FEA and shown in Fig. 7. It is shown that the sum flux linkage of the phase winding can be increased to $\sim$22% by the inner stator. Therefore, the output voltage of DSHESG can also be increased by the same percent.

The phase EMF waveforms of the inner and outer stators against the rotor position are obtained by 3-D FEA at 400 r/min, as shown in Fig. 8(a), which are verified by the measured results [see Fig. 8(b)].

The phase and line EMF waveforms of DSHESG against the rotor position are also obtained by 3-D FEA at 400 r/min, as shown in Fig. 9(a), which has an excellent agreement with the experimental results [see Fig. 9(b)].

According to the flux-linkage method, the inductances of the armature windings and field winding are calculated. The 3-D FEA results of the self-inductance of the armature windings are compared with the measured results in Fig. 10(a), and they are in good agreement. The self-inductance is directly measured by an LCR instrument (HIOKI 3511-50 LCR HiTESTER). Moreover, the mutual inductance between armature windings and field winding against rotor position is computed by FEA, as shown in Fig. 10(b).

IV. Simulated and Measured Results

A. Prototyped DSHESG

The prototyped DSHESG whose design parameters are given in Table I is manufactured, the components of which are shown in Fig. 11. The field winding has 2500 turns with 0.5-mm conductor diameter. There are 120 conductors and 76 conductors in one slot for the outer and inner stators, respectively. The rotor of the DSHESG consists of PMs and claw poles, in which the pole arc width of PMs is 45°. The axis of PMs is in coincidence with that of the corresponding claw poles.

B. Simulation and Experiment

The measured and 3-D FEA-predicted EMF waveforms and winding inductances are already reported in the previous

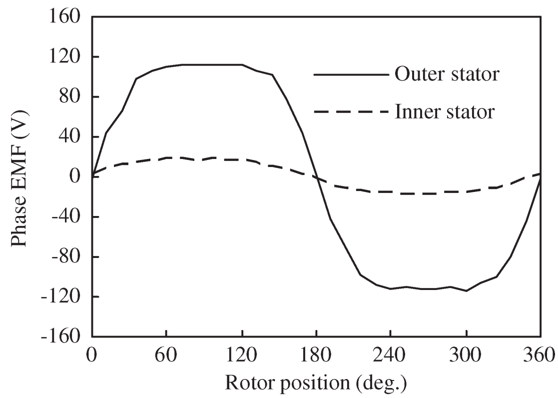

(a)

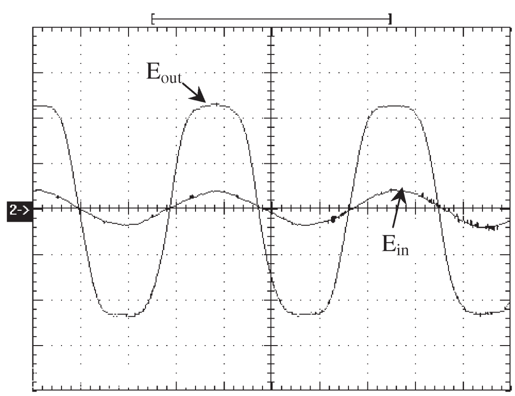

(b)

Fig. 8. Phase EMF waveforms of outer and inner stators at 400 r/min. (a) FEA predicted. (b) Measured (10 ms/div, 50 V/div).

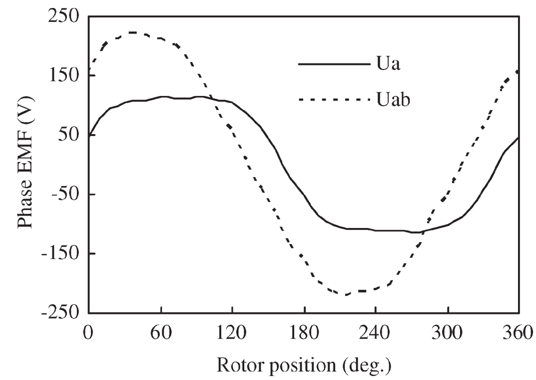

(a)

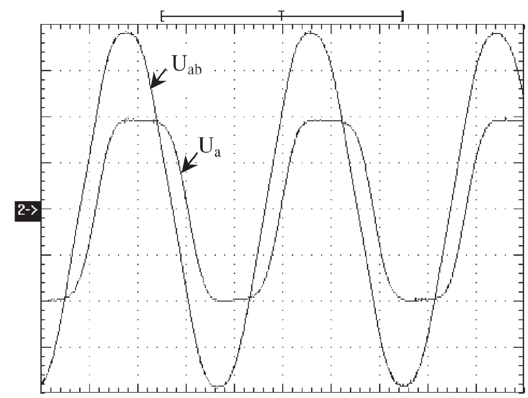

(b)

Fig. 9. Phase and line EMF waveforms of DSHESG at 400 r/min. (a) FEA predicted. (b) Measured (10 ms/div, 60 V/div).

sections, and good agreements have been achieved. In this section, the phase voltage and current waveforms, as well as the air-gap flux, under different field current excitations, are also predicted and measured. Fig. 12 shows the simulated and measured phase voltage and current waveforms with a resistance load at 400 r/min. It shows that they are in good agreement. The simulated results are obtained from the mathematical model of the DSHESG on the MATLAB platform, which is given in the Appendix. The air-gap magnetic fluxes per pole of the DSHESG under different field currents are obtained by FEA and experiment, respectively, as shown in Fig. 13. It indicates that the air-gap magnetic flux per pole at no load can be easily controlled by adjusting the field current from -0.8 to 0.8 A. The experimental result of air-gap flux is acquired by two steps: 1) measuring the phase EMF and 2) calculating the air-gap magnetic flux per pole by (4).

V. CONCLUSION

The structure and operation principle of a novel DSHESG have been described in detail. The magnetic field distributions, flux linkages, winding inductances, and EMF waveforms under different field currents are computed by 3-D FEM. A prototype DSHESG is manufactured, and some experiments are carried out. The FEM and experimental results show that the developed DSHESG has a good capacity of field control, and the power density and the output voltage of the generator can be effectively increased by adopting a dual-stator structure.

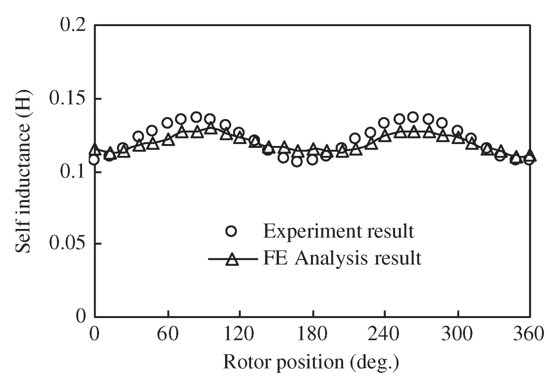

(a)

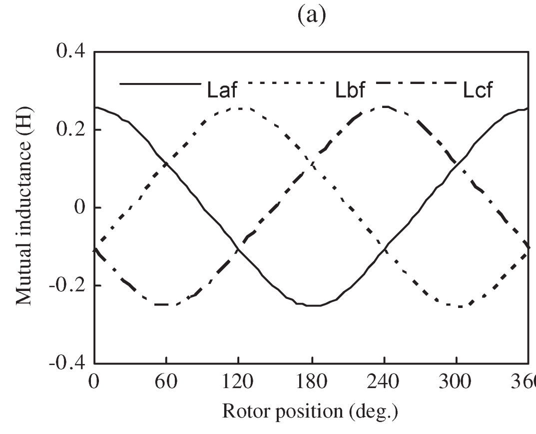

(b)

Fig. 10. Winding inductances. (a) Self-inductance of armature windings. (b) Mutual inductance between armature windings and field winding.

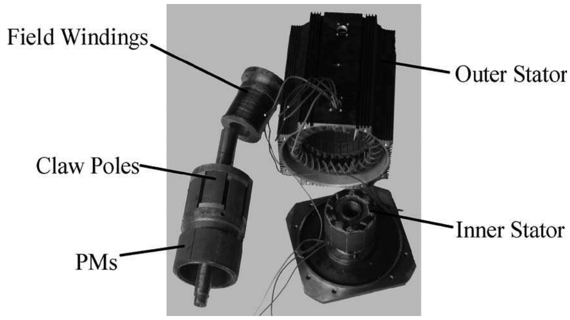

Fig. 11. Prototype of DSHESG.

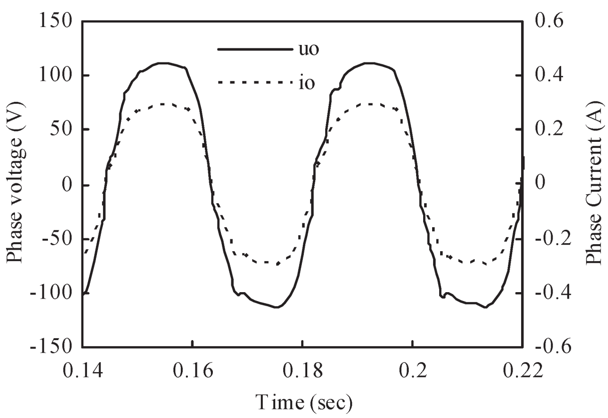

(a)

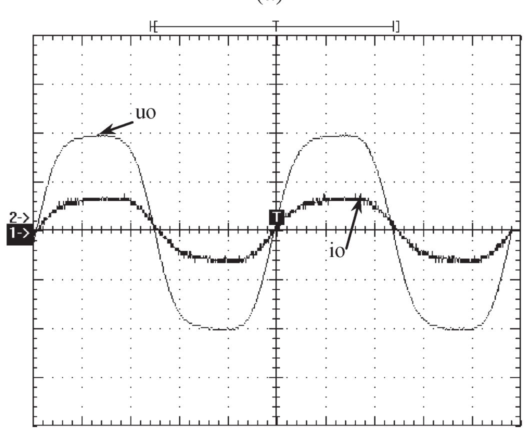

(b)

Fig. 12. Waveforms of phase voltage and current. (a) Simulated. (b) Measured (uo: 7.8 ms/div, 50 V/div; io: 7.8 ms/div, 0.5 A/div).

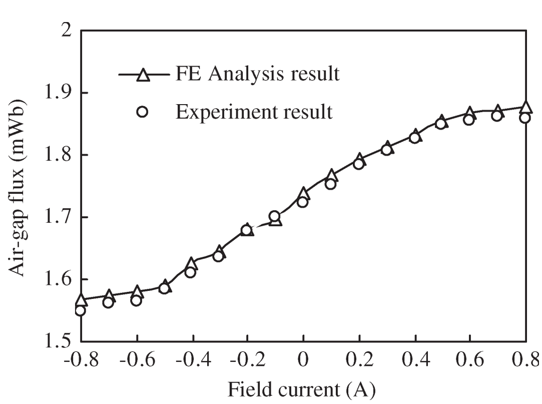

Fig. 13. Waveforms of air-gap magnetic flux per pole.

APPENDIX
MATHEMATICAL MODEL OF DSHESG

The flux-linkage equations of armature windings and field winding of the DSHESG can be expressed as

$$\begin{bmatrix}\Psi_a\\ \Psi_b\\ \Psi_c\\ \Psi_f\end{bmatrix} = \begin{bmatrix} L_{\mathrm{aa}} & M_{\mathrm{ab}} & M_{\mathrm{ac}} & M_{\mathrm{af}}\\ M_{\mathrm{ba}} & L_{\mathrm{bb}} & M_{\mathrm{bc}} & M_{\mathrm{bf}}\\ M_{\mathrm{ca}} & M_{\mathrm{cb}} & L_{\mathrm{cc}} & M_{\mathrm{cf}}\\ M_{\mathrm{fa}} & M_{\mathrm{fb}} & M_{\mathrm{fc}} & L_f\end{bmatrix} \begin{bmatrix} i_a\\ i_b\\ i_c\\ i_f\end{bmatrix} + \begin{bmatrix}\Psi_{\mathrm{pma}}\\ \Psi_{\mathrm{pmb}}\\ \Psi_{\mathrm{pmc}}\\ 0\end{bmatrix} \tag{13}$$

where Ψ_{pm}'s are the flux linkages in the armature windings due to PM magnetic force; Ψ_a, Ψ_b, and Ψ_c are the flux linkages in the three-phase armature windings; Ψ_f is the flux linkage in the field winding; i_a, i_b, and i_c are the three-phase armature currents; i_f is the field current; and L and M denote self-inductance and mutual inductance, respectively.

The circuit equations of all windings can be expressed as

$$\boldsymbol{U} = \boldsymbol{RI} + \frac{d\boldsymbol{\Psi}}{dt} \tag{14}$$

where $\boldsymbol{U} = [u_a \quad u_b \quad u_c \quad u_f]^{\mathrm{T}}$, $\boldsymbol{I} = [i_a \quad i_b \quad i_c \quad i_f]^{\mathrm{T}}$, $\boldsymbol{R} = \mathrm{diag}[-r_a \quad -r_b \quad -r_c \quad r_f]$, and $\boldsymbol{\Psi} = [\Psi_a \quad \Psi_b \quad \Psi_c \quad \Psi_f]^{\mathrm{T}}$.

REFERENCES

[1] A. Shakai, Y. Liao, and T. A. Lipo, "A permanent magnet AC machine structure with true field weakening capability," in *Proc. IEEE-ISIE*, Budapest, Hungary, Jun. 1–3, 1993, pp. 19–24.

[2] F. Leonardi, T. Matsuo, Y. Liao, and T. A. Lipo, "Design considerations and test results for a doubly salient PM motor with flux control," in *Conf. Rec. IEEE IAS Annu. Meeting*, San Diego, CA, Jan. 6–10, 1996, pp. 458–463.

[3] J. A. Tapia, F. Leonardi, and T. A. Lipo, "Consequent-pole permanent-magnet machine with extended field-weakening capability," *IEEE Trans. Ind. Appl.*, vol. 39, no. 6, pp. 1704–1709, Nov./Dec. 2003.

[4] C. C. Chan, K. T. Chau, and J. Z. Jiang, "Novel permanent magnet motor drives for electric vehicles," *IEEE Trans. Ind. Electron.*, vol. 43, no. 2, pp. 331–339, Apr. 1996.

[5] L. Video and M. Gabsi, "Homopolar and bipolar hybrid excitation synchronous machines," in *Conf. Rec. IEEE-IEMDC*, San Antonio, TX, May 15–18, 2005, pp. 1212–1218.

[6] Z. G. Liang, Y. L. Xu, R. Y. Tang, and Y. Hu, "3D magnetic field analysis of a hybrid excitation synchronous generator," in *Proc. IEEE-ICEMS*, Shenyang, China, Aug. 18–20, 2001, pp. 164–166.

[7] Y. Y. Ni, Q. J. Wang, and X. H. Bao, "Optimal design of a hybrid excitation claw-pole alternator," in *Proc. IEEE-ICEMS*, Nanjing, China, Sep. 27–29, 2005, pp. 644–647.

[8] N. Naoe and T. Fukami, "Trial production of a hybrid excitation type synchronous machine," in *Conf. Rec. IEEE-IEMDC*, Cambridge, MA, Jun. 17–20, 2001, pp. 545–547.

[9] J. F. Eastham, P. D. Evans, and P. C. Coles, "Double disc alternators with hybrid excitation," *IEEE Trans. Magn.*, vol. 28, no. 5, pp. 3039–3041, Sep. 1992.

[10] F. Tomas and H. Kay, "Study and geometry optimization of hybrid excited synchronous alternators for automotive applications," in *Conf. Rec. IEEE-IEMDC*, Antalya, Turkey, May 3–5, 2007, pp. 124–128.

[11] F. Chai, S. M. Cui, and S. K. Cheng, "Performance analysis of double-stator starter generator for the hybrid electric vehicle," *IEEE Trans. Magn.*, vol. 41, no. 1, pp. 484–487, Jan. 2005.

[12] S. X. Niu, K. T. Chau, J. Z. Jiang, and C. H. Liu, "Design and control of a new double-stator cup-rotor permanent-magnet machine for wind power generation," *IEEE Trans. Magn.*, vol. 43, no. 6, pp. 2501–2503, Jun. 2007.

[13] D. Zhang, K. T. Chau, S. X. Niu, and J. Z. Jiang, "Design and analysis of a double-stator cup-rotor PM integrated-starter-generator," in *Conf. Rec. IEEE IAS Annu. Meeting*, Tampa, FL, Oct. 8–12, 2006, pp. 20–26.

[14] B. Q. Kou, L. Y. Li, S. K. Cheng, and F. R. Meng, "Torque characteristics of double-stator hybrid stepping motor with serial magnetic circuit structure," in *Conf. Rec. IEEE-IEMDC*, Madison, WI, Jun. 1–4, 2003, pp. 313–318.

[15] M. Mirsalim, M. Mirzaei, and H. Bahrami, "A novel high-speed flux reversal alternator," in *Conf. Rec. IEEE-PEMD*, Dublin, Ireland, Apr. 4–6, 2006, pp. 212–215.

[16] P. P. Acarnley, B. C. Mecrow, J. S. Burdess, J. N. Fawcett, J. G. Kelly, and P. G. Dickinson, "Design principles for a flywheel energy store for road vehicles," *IEEE Trans. Ind. Appl.*, vol. 32, no. 6, pp. 1402–1408, Nov./Dec. 1996.

[17] O. Ojo and I. E. Davidson, "PWM-VSI inverter-assisted stand-alone dual stator winding induction generator," *IEEE Trans. Ind. Appl.*, vol. 36, no. 6, pp. 1604–1611, Nov./Dec. 2000.

[18] Y. Kano, K. Tonogi, T. Kosaka, and N. Matsui, "Torque-maximizing design of double-stator, axial-flux, PM machines using simple non-linear magnetic analysis," in *Conf. Rec. IEEE IAS Annu. Meeting*, New Orleans, LA, Sep. 23–27, 2007, pp. 875–881.

[19] Y. Amara, J. Lucidarme, and M. Gabsi, "A new topology of hybrid synchronous machine," *IEEE Trans. Ind. Appl.*, vol. 37, no. 5, pp. 1273–1281, Sep./Oct. 2001.

[20] Y. S. Chen, Z. Q. Zhu, and D. Howe, "Calculation of d- and q-axis inductances of PM brushless ac machines accounting for skew," *IEEE Trans. Magn.*, vol. 41, no. 10, pp. 3940–3942, Oct. 2005.

Xiping Liu received the B.S. degree from Hohai University, Nanjing, China, in 1999, the M.S. degree from Jiangxi University of Science and Technology, Ganzhou, China, in 2004, and the Ph.D. degree in electrical engineering from Southeast University, Nanjing, China, in 2009.

From 1999 to 2009, he was a Lecturer in the School of Mechanical and Electrical Engineering, Jiangxi University of Science and Technology. He is involved in the analysis and design of permanent-magnet synchronous machines and wind power technology.

Heyun Lin received the B.S., M.S., and Ph.D. degrees in electrical engineering from Nanjing University of Aeronautics and Astronautics, Nanjing, China, in 1985, 1989, and 1992, respectively.

From 1992 to 1994, he was a Postdoctoral Fellow at Southeast University, Nanjing, China. In 1994, he joined the School of Electrical Engineering, Southeast University, as an Associate Professor. He became a Full Professor in 2000. His main research is related to the design, analysis, and control of permanent-magnet motors, intelligent electrical apparatus, and electromagnetic field numerical analysis. He is the author of more than 60 technical papers and the holder of ten patents.

Prof. Lin is a member of the Electrical Motor and Apparatus Committee of Jiangsu Province and a Senior Member of both the China Society of Electrical Engineering and the China Electrotechnical Society.

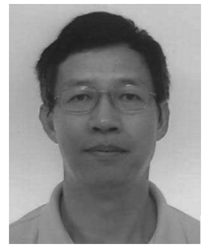

Z. Q. Zhu (M'90–SM'00–F'09) received the B.Eng. and M.Sc. degrees from Zhejiang University, Hangzhou, China, in 1982 and 1984, respectively, and the Ph.D. degree from the University of Sheffield, Sheffield, U.K., in 1991, all in electrical and electronic engineering.

From 1984 to 1988, he was a Lecturer with the Department of Electrical Engineering, Zhejiang University. Since 1988, he has been with the University of Sheffield, where he was initially a Research Associate and was subsequently appointed to an established post as Senior Research Officer/Senior Research Scientist in 1992. Since 2000, he has been a Professor of Electrical Machines and Control Systems with the Department of Electronic and Electrical Engineering, University of Sheffield, and is currently Head of the Electrical Machines and Drives Research Group. His current major research interests include applications, control, and design of permanent-magnet machines and drives.

Chengfeng Yang received the B.S. and M.S. degrees from Hohai University, Nanjing, China, in 1997 and 2002, respectively, and the Ph.D. degree from Southeast University, Nanjing, China, in 2008, all in electrical engineering.

His primary areas of interest are electromechanical analysis and electrical machine design for ac adjustable-speed applications, and magnetic field analysis.

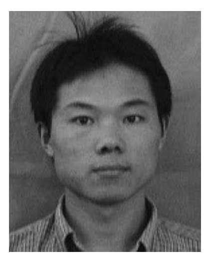

Shuhua Fang received the M.S. degree from Shandong University of Science and Technology, Jinan, China, in 2004, and the Ph.D. degree from Southeast University, Nanjing, China, in 2008, both in electrical engineering.

From 1998 to 2001, he was an Associate Engineer with the Xuzhou Coal and Mine Machinery Factory, where his research activities were primarily in the area of the design, analysis, and control of electrical apparatus for coal and mines. He joined the School of Electrical Engineering, Southeast University, as a Lecturer in 2008. His research interests include intelligent apparatus design, simulation, and control.

Jian Guo received the M.S. degree from Shenyang University of Technology, Shenyang, China, in 2005, and the Ph.D. degree from Southeast University, Nanjing, China, in 2008, both in electrical engineering.

He joined the College of Automation Engineering, Nanjing University of Aeronautics and Astronautics, Nanjing, China, as a Lecturer in 2008. His main research is related to the design of power transformers and electromagnetic field numerical analysis.